



## Original contribution

# Co-expression of cytokeratin and vimentin in colorectal cancer highlights a subset of tumor buds and an atypical cancer-associated stroma ☆, ☆ ☆, ★



Sara N. Meyer MD<sup>a,1</sup>, José A. Galván PhD<sup>a,1</sup>, Stefan Zahnd PhD<sup>a</sup>, Lena Sokol PhD<sup>a,b</sup>, Heather Dawson MD<sup>a</sup>, Alessandro Lugli MD<sup>a</sup>, Inti Zlobec PhD<sup>a,\*</sup>

<sup>a</sup>Institute of Pathology, University of Bern, Murtenstrasse 31, Bern, CH-3008, Switzerland

<sup>b</sup>Swiss Group for Clinical Cancer Research, Effingerstrasse 33, Bern, CH-3008, Switzerland

Received 3 October 2018; revised 11 January 2019; accepted 4 February 2019

## Keywords:

Colorectal cancer;  
Tumor budding;  
Cancer-associated stroma;  
Epithelial-mesenchymal transition;  
Mesothelial-mesenchymal transition

**Summary** Tumor buds in colorectal cancer are hypothesized to undergo a (partial) epithelial-mesenchymal transition (EMT). If so, cytokeratin (CK) and vimentin (VIM) co-expression is expected. CK+/VIM+ can also be found in some stromal cells; however, their origin remains unclear. Here, we determine the frequency of CK+/VIM+ tumor cells and characterize the CK+/VIM+ stroma in colorectal cancer. Three cell populations (CK+, VIM+, CK+/VIM+) were sorted using DepArray and fluorescence-activated cell sorting (FACS). Tumor areas were selected to include tumor center, stroma and tumor budding. Fluorescence microscopy was used to visualize co-expressing cells on whole slides. A next-generation tissue microarray (ngTMA) of matched Pan-CK–positive and -negative stroma was constructed and stained for E-cadherin, VIM, Snail1, Twist1, Zeb1 and Zeb2, COL11A1, SPARC, CD90,  $\alpha$ -SMA, FAP and WT1. CK+/VIM+ co-expressing tumor cells were detected using all three methods. With DepArray, only tumor budding areas contained CK+/VIM+ cells. The proportion of CK+/VIM+ tumor cells was low (1.5%–22%). CK+ stroma was associated with aggressive tumor features like distant metastasis ( $P = .0003$ ), lymphatic invasion ( $P = .0009$ ) and tumor budding ( $P = .0084$ ). CK+/VIM+ stroma was characterized by positive WT1 ( $P < .001$ ), ZEB2 ( $P < .001$ ), TWIST1 ( $P = .009$ ), and FAP ( $P = .003$ ). Our data suggest that CK+/VIM+ tumor cells exist, albeit in low numbers and could represent a subgroup of tumor buds in partial EMT. CK+/VIM+ stroma may be of mesothelial origin and shows features of mesenchymal cells and cancer-associated fibroblasts. These results, together with the association with metastasis point to cells in mesothelial-mesenchymal transition (MMT). This atypical stroma may be a potential target for therapy.

© 2019 Elsevier Inc. All rights reserved.

☆ Competing interests: the authors have no disclosures or conflicts of interest.

☆☆ Funding/Support: We thank the Werner und Hedy Berger Janser Stiftung, as well as the Mach-Gaensslen Stiftung and Johanna Dürmüller-Bol foundation for supporting this work.

★ Declaration of interest: none.

\* Corresponding author at: University of Bern, Institute of Pathology, Murtenstrasse 31, Bern, CH-3008, Switzerland.

E-mail address: [inti.zlobec@pathology.unibe.ch](mailto:inti.zlobec@pathology.unibe.ch) (I. Zlobec).

<sup>1</sup> Authors contributed equally.

## 1. Introduction

Tumor budding in colorectal cancer is recognized as an important prognostic factor [1]. The presence of tumor buds, defined as single tumor cells or small tumor cell clusters (up to 4 cells), leads to worse overall and disease-free survival and is associated with advanced tumor stage, lymphatic and venous invasion as well as lymph node and distant metastasis.

Tumor budding has often been referred to as a hallmark of epithelial-mesenchymal transition (EMT) but the morphology of tumor buds, as well as immunohistochemistry and RNA profiles do not suggest a full transition to a mesenchymal state [2,3]. A closer look at tumor budding in the literature suggests that only a subset of tumor buds shows nuclear expression of  $\beta$ -catenin and absence of membranous E-cadherin, which are considered “classic” signs of EMT, but this differs between tumor types (eg, more frequently found in colorectal cancers but almost never reported in pancreatic ductal adenocarcinoma) [3-7].

On the other hand, laser capture microdissection studies in both colorectal cancers and oral squamous cell carcinomas show an up-regulation of EMT-related genes in regions capturing tumor buds [8,9]. For example, De Smedt and colleagues report a shift from an epithelial profile in the tumor center to a more mesenchymal one in regions that have captured tumor buds [8]. Our group has also recently shown an association between high-grade tumor budding and the mesenchymal/poor prognostic subgroup of the Consensus Molecular Subtypes (CMS4) characterized by up-regulation of matrix remodeling genes, as well as EMT- and cancer stem cell-related genes [10,27]. Interestingly, the presence of cytokeratin (CK) is often used as a marker for the visualization of tumor budding, which as a marker for epithelium inherently contradicts the EMT hypothesis [11]. Some authors refer to “partial” EMT, which suggests a hybrid state in which epithelial and mesenchymal conditions can simultaneously be observed [2].

If partial EMT exists, then tumor cells with both epithelial and mesenchymal characteristics, for example, expressing both CK and vimentin (VIM) should be detectable. We hypothesize therefore that a subset of tumor buds is in fact in a state of partial EMT, which can be observed by co-expression of both CK and VIM.

However, tumor cells are not the only double-positive cell type in colorectal cancers. Fibroblasts proximal to the mesothelium are also immunoreactive to CK and VIM by immunohistochemistry. Until now, this type of stromal reaction has simply been dismissed as “reactive” but has not been well-characterized. Chen and Borges show that local peritoneal injury associated with tumor invasion is characterized by activation and proliferation of serosal stromal cells that express CK and mesothelial cell-like features in gastrointestinal tumors [12]. The degree of this stromal proliferation is associated with the degree of injury, extent of tumor invasion and type of tumor. Other studies have postulated that during peritoneal metastasis, the mesothelium is replaced by a strong stromal reaction, characterized by activated myofibroblasts, in a process named mesothelial-mesenchymal transition (MMT) [13,14]. These fibroblasts have been considered by several authors as CAF (Cancer-Associated Fibroblasts) which promote tumor progression through communication with cancer cells [15-17]. However, there are multiple theories about the origin of CAFs which are still unclear.

The aims of this study are (1) to determine whether CK/VIM co-expressing tumor cells exist in colorectal cancer and whether these cells can be attributed to a subgroup of

tumor buds and (2) to characterize the CK-expressing stroma and its association with clinicopathologic features in patients with colorectal cancer.

## 2. Materials and methods

### 2.1. Patient cohort

Consecutive surgically treated colorectal cancer cases from 2013 to 2015 ( $n = 208$ ) were retrospectively selected for this study. During this period of time, CK immunohistochemistry using a pan-CK antibody (AE1/AE3) was standard practice at our institute for the detection and quantification of tumor budding, making CK-stained slides readily available. Clinicopathologic information was obtained from diagnostic charts and included the following parameters: gender, age at diagnosis, TNM classification, venous (V) and lymphatic (L) vessel invasion, perineural (Pn) invasion, R classification, tumor grade, Klintrup-Mäkinen score, number of tumor buds in 10 high-power fields (HPFs) assessed using AE1/AE3-stained whole tissue slides [18] and the percentage of expansive (pushing) tumor border. The total number of lymph nodes and number of positive lymph nodes was also recorded. No preoperatively treated cases were included in this study. This cohort was used to detect the association of CK-positive stroma with histopathological features.

### 2.2. Digital annotations for selection of regions for DepArray analysis

From these 208 cases, five cases with the greatest amount of tumor buds counted on CK staining across 10 HPFs were selected for digital annotation. The formalin-fixed paraffin-embedded tissue block corresponding to each case was retrieved from the archives of the Institute of Pathology, University of Bern and a fresh section and immunohistochemistry for AE1/AE3 was made. This slide was then scanned (P250, 3DHitech, Budapest) and annotated in the following manner using a tissue microarray annotation tool: yellow, red/orange and green representing tumor center, tumor budding and stroma proximal to the tumor. Using a tissue microarraying instrument (TMA Grandmaster; 3DHitech, Budapest, Hungary), blocks were loaded into the machine, and the corresponding annotated CK scan was aligned to an image of each block [19]. Annotated regions were cored out using a 0.6 mm or 1.0 mm tool and tissues were placed into separate 0.2 mL tubes. This technology allowed us to specifically select regions of tumor budding and compare staining and mutational profiles of these areas with the tumor and stroma environment.

### 2.3. DepArray analysis and next-generation sequencing

In order to determine the existence, frequency and origin of CK+/VIM+ cells in the tumor budding population, we chose a

DepArray method (Silicon Biosystems, Bologna) [20]. Briefly, samples in tubes were sent to Silicon Biosystems, where they were deparaffinized and disaggregated into a single cell suspension. Next, heat-induced epitope retrieval and immunofluorescence labeling for CK-Alexa488, VIM-Alexa647 and DAPI were performed. The stained single cell suspension was pipetted into a microfluidic silicon-biochip single use cartridge, where the single cells were distributed into individual di-electrophoresis chambers, and inserted into the DEPArray instrument. The trapped cells of interest (ie, cells positive for DAPI, VIM, and CK) could be individually selected, separated by di-electrophoresis, counted and recovered. In a last step, next-generation sequencing was performed on the recovered cells using the Ion AmpliSeq Cancer Hotspot Panel v2 and analyzed with TorrentSuite v4.4 (Thermo Fischer).

## 2.4. Fluorescence-activated cell sorting

Tissues from 6 colorectal cancers were carefully selected for fluorescence-activated cell sorting (FACS) analysis. Blocks were chosen such that no normal tissue, fat, mucinous components or CK-positive stromal areas were included in the blocks. Nine 50  $\mu$ m tissue rolls were cut and packed into nylon biopsy bags to prevent cell loss. Deparaffinization was performed in a large volume of xylol, followed by rehydration in decreasing percentages of ethanol. Antigen retrieval was performed in citrate buffer for 2 hours at 80°C. The tissue was enzymatically dissociated for 60 min in RPMI containing 0.2% collagenase Ia and dispase. Antibody labelling was performed using CK (MNF116 – Dako and AE1/AE3 – Millipore) and VIM (3B4 – Dako) as primary, and AF488 IgG1 and AF647 IgG2a (Life Technologies) as secondary antibodies. Additionally, the nucleus was labeled with DAPI.

## 2.5. Matched CK-positive and CK-negative ngTMA

Eighty-nine mixed stage colon cancers cases with CK-positive stroma, treated at the Department of Surgery at the Technical University Munich hospital, Munich, Germany, between 1993 and 2005 were included in this part of the study. A next-generation tissue microarray (ngTMA) of matched CK-positive and negative stromal areas was constructed [19] (Supplementary Fig. 1). Briefly, the CK slide was scanned and annotated using a TMA tool of 0.6 mm diameter in one area of CK positivity and one area of negativity. The annotated scans were then aligned to the image of the donor block and the precise area was cored out for ngTMA construction. The end result was a matched CK-positive and negative ngTMA used for subsequent analysis of stromal markers by immunohistochemistry.

## 2.6. Immunofluorescence and confocal microscopy

In order to visualize the epithelial and mesenchymal double-positivity of tumor buds on, a fluorescence staining protocol was developed. This immunofluorescence staining was applied

to whole tissue slides from the five cases sent for DepArray analysis as well as the tumor invading vessel ngTMA. Slides were cut at 2.5  $\mu$ m. Fluorescent labelling was performed on the Bond RX (Leica Microsystems). Antigen retrieval with citrate buffer at 100°C for 30 min was applied. Subsequently, we applied 0.2% (v/v) Triton X-100 in 1 $\times$  phosphate-buffered saline (PBS) for 20 min. The blocking step was implemented using 1% bovine serum albumin (w/v) and 5% horse serum (w/v) for 20 min. Primary antibodies (listed in Supplementary Table 1), mouse pan-CK (AE1/AE3) antibody with rabbit VIM antibody and mouse E-cadherin antibody with rabbit VIM antibody were incubated for 60 min. Goat anti-rabbit Alexa Fluor 488 and goat anti-mouse Alexa Fluor 546 (Invitrogen), were used as secondary antibodies, in a dilution of 1:1000 for both antibodies, for 60 min. Mounting medium with DAPI (Vectashield). Images were taken on an Olympus FluoView-1000 (Olympus) confocal microscope at 60 $\times$  magnification.

## 2.7. Immunohistochemistry

Single and double immunohistochemistry was performed on the Bond RX (Leica Microsystems) on the matched stroma ngTMA for the following makers: (1) E-cadherin and VIM in order to determine the epithelial and mesenchymal origin respectively; (2) Snail1, Twist1, Zeb1 and Zeb2 to determine the activated EMT/mesothelial-mesenchymal transition (MMT) process; (3) COL11A1, SPARC, CD90,  $\alpha$ -SMA, and FAP to determine the “CAF/myofibroblast” phenotype; (4) WT1 determine mesothelial phenotype. In addition, whole tissue slides from one tumor with CK-positive stroma and known *BRAF* V600E mutation underwent immunohistochemistry for the VE1 antibody and CK20. This was performed in order to determine whether the CK-positive stroma derived from the tumor itself. All primary antibodies and protocols are listed in Supplementary Table 1. All single stainings as well as the first step in double stainings were visualized with Bond polymer refine detection, using 3,3'-diaminobenzidine (DAB) as brown chromogen (Leica Biosystems). The second step of double stainings were visualized with Red polymer refine Detection, using fast red as red chromogen (Leica Biosystems, Ref DS9390). Finally, the samples were counterstained with hematoxylin and mounted with Aquatex (Merck). Slides were scanned using Panoramic P250 (3DHitech, Budapest).

## 2.8. Ethics

Ethical approval was obtained for the use of all tissue and data in this study (KEK# b2017–01803).

## 2.9. Statistical analysis

Associations between CK status in stroma and categorical clinicopathologic features was performed using the  $\chi^2$  test or Wilcoxon rank-sum test for continuous variables. A

matched-pairs analysis using McNemar test was carried out to test stroma expression differences.  $P < .05$  was considered statistically significant. Analyses were carried out using SPSS v24 (IBM, New York, NY) and SAS, v9.2 (SAS Institute, Cary, NC).

### 3. Results

#### 3.1. DepArray analysis reveals a small population of CK+/VIM+ co-expressing cells

Three different tissue areas were investigated for single and double-positive cells: the tumor center, tumor stroma and areas of tumor budding at the invasion front. These areas were punched out from the corresponding tissue blocks of five cases and sent separately for DepArray analysis. The number of investigated double or single positive cells in each of the three compartments (center: CK only and CK/VIM; stroma: VIM only and CK/VIM; tumor budding: CK only and CK/VIM) was quantified.

Out of 5 samples, disaggregation was successful in four and of these, all could be successfully analyzed in the center, stroma and tumor budding regions except in sample 4 budding region. In areas of the tumor center and the stroma, only CK+ and VIM+ single cells were identified, respectively. Tumor budding regions from three samples contained CK+ single cells while two different samples showed CK+/VIM+ double-positive cells. The frequency of CK+/VIM+ double-positive cells was 10/337 (2.9%) in sample 1 and 49/173 (22%) in sample 3. Whole tissue slides of these cases stained for CK and VIM were also examined by fluorescent and confocal microscopy and found to contain CK+/VIM+ single cells or small tumor cell clusters (Fig. 1).

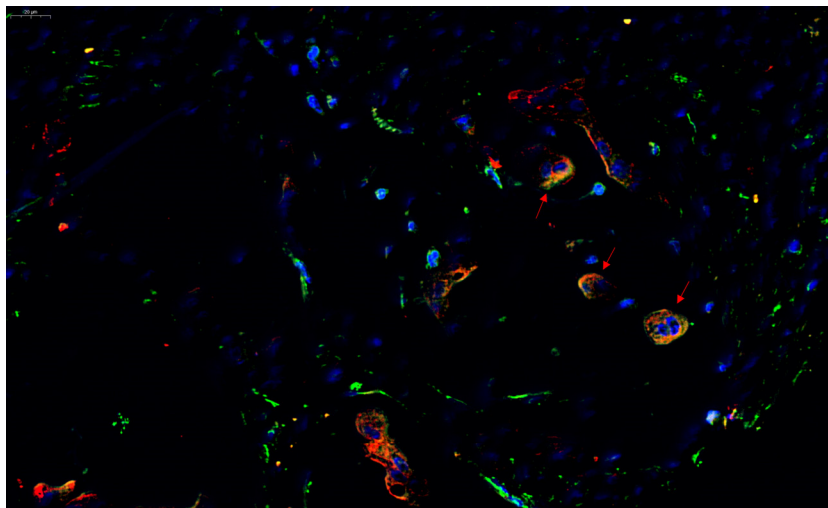
#### 3.2. Next-generation sequencing of double-positive tumor cells

In order to verify that the double-positive cells were of tumor origin, we performed next-generation sequencing using an ion Torrent 50 gene cancer panel. Due to the low input of DNA, only one sample could be successfully sequenced. The mutational profile of the double-positive cells was compared to that of the corresponding tumor center and to the proximal stroma (Table 1).

Four mutations were identified in the double-positive population: *BRAF*<sup>V600E</sup> missense, *PTEN* deletion, *TP53* missense G>V and a second *TP53* P>R missense mutation. Importantly, the mutated allele frequency was 100% for *BRAF* V600E in the CK+ cells of the tumor center and 100% in both the CK+ only and CK+/VIM+ cells of the tumor budding population but 0% in the proximal tumor stroma. Similar results were found for *PTEN* deletion and *TP53* G>V with the same aberrations found in the tumor center as well as both CK+ and CK+/VIM+ tumor budding area cell collection, but not in the tumor stroma. The final mutation is *TP53* P>R was mutated in all tissue areas suggesting its non-sporadic origin.

#### 3.3. FACS sorting of single and double-positive tumor cells

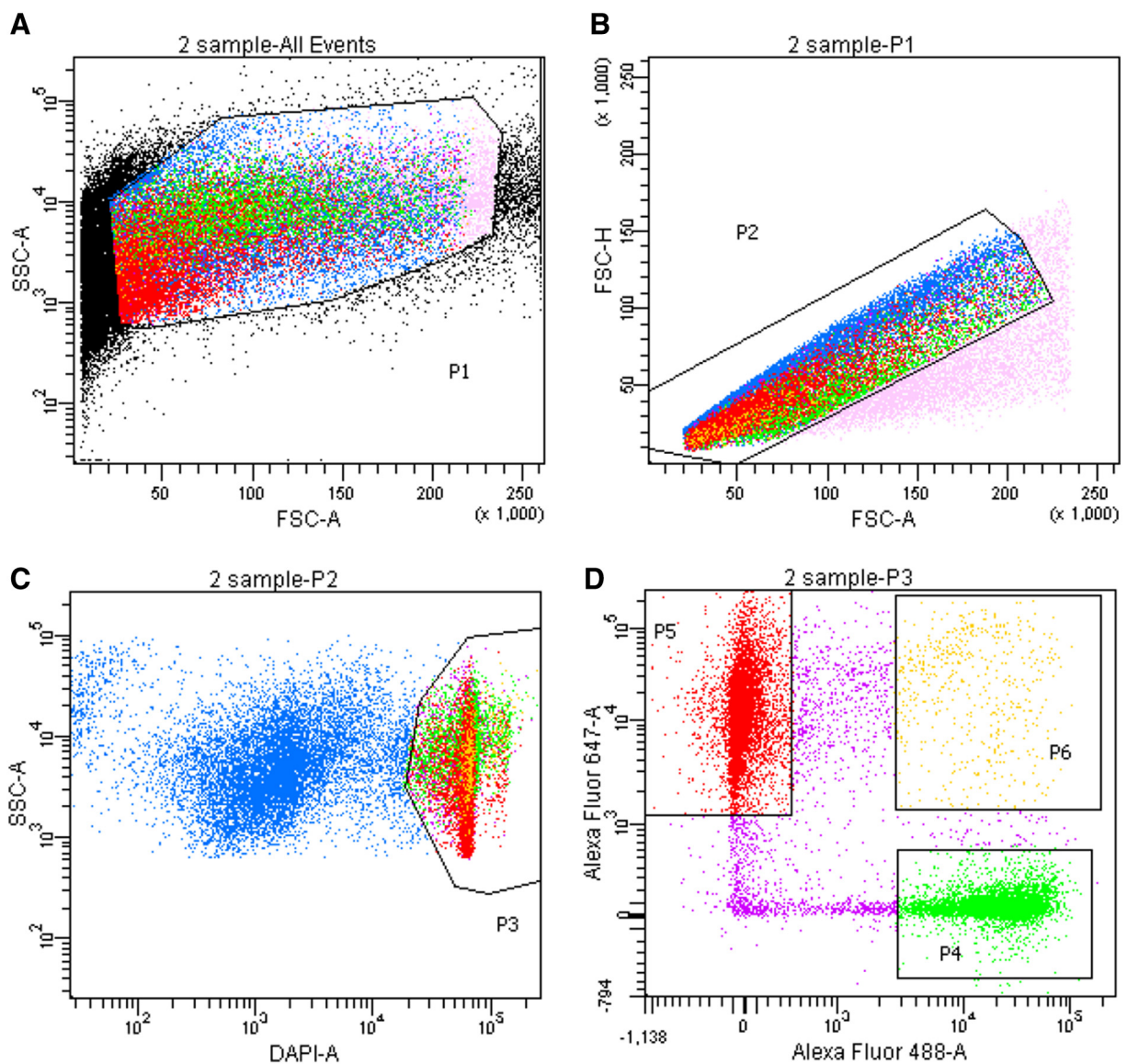
Six tumor samples were sorted for CK+, VIM+ and CK+/VIM+ double-positive cells. On average the tissue contained 26% CK+ and 42% VIM+ cells (Fig. 2). To ensure maximal purity and exclude the possibility of doublets, the VIM+/CK+ double-positive cells were subsequently re-sorted. Using this protocol, of all CK-positive cells sorted, approximately 1.5% were determined to be double-positive for CK+/VIM+ (Table 2).



**Fig. 1** Immunofluorescence staining of colorectal cancer using pan-CK (AE1/AE3) (red) and VIM (green). Red arrows point to CK/VIM co-expressing tumor buds.

**Table 1** Mutational profile of double-positive cells in comparison to tumor center and stromal compartments following next-generation sequencing

Gene	Ref	Alt	Invasion front			Tumor center	Mutation type	Variant designation
			Stroma CK-VIM+ N = 283	CK+VIM- N = 300	CK+VIM+ N = 10	CK+VIM- N = 286		
<i>BRAF</i>	A	T	0%	100%	100%	100%	V600E missense	Exon 15 c.1799T>A
<i>PTEN</i>	G	A	0%	Lost	Lost	Lost	Gene deletion	
<i>TP53</i>	T	A	0%	100%	100%	100%	Missense	Exon 5 c.536A>T
<i>TP53</i>	G	C	91%	100%	92%	100%	Missense	Exon 4 c.215C>G

**Fig. 2** Gating in FSC-A/SSC-A (A, P1) was performed to remove debris, in FSC-A/FSC-H to exclude fused cells (B, P2), and DAPI staining was used to help select intact cells containing both a nucleus and cytoplasm (C, P3). In panel D, CK+ (P4), VIM+ (P5), and CK+VIM+ cell populations are shown.

**Table 2** Number of VIM-positive, CK sorted, and CK+/VIM+ double-positive sorted cells in six tumor samples

Tumor #	VIM+ cell number	VIM+ %	CK+ cell number	CK+ %	CK+/VIM+ cell number	CK+/VIM+ % of all CK+
1	373 321	58.2	133 798	11.9	2237	1.6%
2	1 247 618	28.5	323 220	8.1	5449	1.7%
3	1 303 164	45.1	838 025	29.8	5404	0.6%
4	648 009	22.1	1 395 579	48.3	33 209	2.3%
5	1 352 710	38.2	1 349 411	41.0	10 769	0.8%
6	764 766	60.2	282 818	20.8	7078	2.4%
Average		42.1		26.7		1.6%
SD		15.5		16.0		0.7

Next, to confirm the purity and verify the origin of the double-positive cells, a mutation test was performed on all sorted populations (Hotspot 50-gene cancer panel). As expected, no mutations were detected in VIM+ cell populations, whereas the CK+/VIM+ double-positive population contained the same mutations as the CK+ tumor cell population (*PIKCA*, *TP53*).

### 3.4. CK-positive stroma and clinicopathologic features

The clinicopathologic associations of the CK-positive stroma were investigated on 208 colorectal cancer cases. CK stroma was positive in 89 (42.8%) of cases and associated with numerous features of aggressive tumor behavior, including more advanced pT classification ( $P < .0001$ ) and lymph node metastases ( $P = .0402$ ), the presence of venous ( $P = .0119$ ) and lymphatic vessel invasion ( $P = .0009$ ) (Table 3). Patients with CK-positive stroma were also much more likely to have a synchronous metastasis ( $P = .0003$ ) and a significantly greater number of tumor buds counted across 10 HPFs.

### 3.5. Immunohistochemistry characterization of CK-positive stroma

In a first step, immunohistochemistry staining for CK20 and the VE1 antibody detecting the mutant BRAF<sup>V600E</sup> protein was stained in a known BRAF-mutated case with CK stroma. While the tumor was strongly positive for both proteins, the CK stroma area was negative.

Second, we evaluated the CK-positive stroma and its matched negative (cancer-associated) counterpart for different markers including CD90, FAP, SPARC, COL11A1, WT1, ZEB1, ZEB2, SNAIL1 and TWIST1. Results are found in Table 4. The CK-positive stroma was characterized by significantly greater expression of FAP ( $P = .003$ ), WT1 ( $<0.0001$ ), ZEB2 ( $P < .0001$ ) and TWIST1 ( $P = .009$ ) (Fig. 3). All cases of CK-positive and negative stroma were positive for ZEB1 while 53/55 (96.4%) and 49/57 (89.1%) of CK-negative and CK-positive cases, respectively were positive for CD90. In 3 representative cases, we performed double immunostaining using CK, VIM and  $\alpha$ -SMA combined with Snail1, Twist1 and Zeb2. We found that in CK-positive

stroma, the signal from transcription factors came from these fibroblasts (Fig. 4).

## 4. Discussion

The novel findings of this study show that indeed CK and VIM double-positive tumor cells exist in colorectal cancer and that these cells may indeed be a subgroup of tumor buds. In addition, we highlight that the CK-positive reactive stroma is associated with more aggressive tumor behavior and can be characterized as an atypical cancer-associated stroma.

In a first step, we investigated the frequency and mutational status of CK/VIM double-positive tumor cells in colorectal cancer. Samples from the tumor center, tumor budding, and nearby stroma were analyzed for the presence of single expression and double-positive co-expression. We were able to collect specific areas of high-grade tumor budding by using a digital pathology-based approach [28]. Namely a scanned CK stained slide was annotated using a tissue microarray tool; however, punched cores were collected into tubes for downstream analysis by DepArray [19,20]. Double-positive cells were observed in 2 out of the 4 samples that could be analyzed and were only found in samples with tumor buds. Of all CK-positive cells collected among the tumor budding regions, 3%–22% co-expressed VIM. In addition, to verify the origin of these double-positive cells, NGS analysis revealed a mutational profile that was completely concordant with that of the tumor center. These results not only confirm the existence of a cell type displaying both epithelial and mesenchymal features but also strongly suggests that these cells are in fact tumor buds. Confocal microscopy of co-stained whole tissue slides for CK and VIM as well as CK and E-cadherin also clearly highlights the presence of isolated tumor cells expressing both proteins. Moreover, we established a protocol for FACS sorting of cells from FFPE colorectal cancers. Again here we found that approximately 3% of all CK-positive cells also co-expressed VIM. Although these results do not prove that tumor buds are per se contributing to this double-positive phenotype, our FACS findings nonetheless highlight the existence of such a hybrid cell phenotype in colorectal cancer.

**Table 3** Association of the presence of a CK-positive stroma and clinicopathologic features of colorectal cancer patients (n = 208)

Feature		CK-positive stroma N (%)		P
		Negative (n = 129)	Positive (n = 89)	
Gender (n = 208)	Male	73 (61.3)	55 (61.8)	.947
	Female	46 (38.7)	34 (38.2)	
pT classification (n = 208)	pT1	22 (18.5)	1 (1.1)	<.0001
	pT2	21 (17.7)	6 (6.7)	
	pT3	55 (46.2)	46 (51.7)	
	pT4	21 (17.6)	36 (40.5)	
pN classification (n = 195)	pN0	69 (65.1)	45 (50.6)	.0402
	pN1–2	37 (34.9)	44 (49.4)	
V classification (n = 204)	V0	82 (70.1)	46 (52.9)	.0119
	V1–2	35 (29.9)	41 (47.1)	
L classification (n = 206)	L0	65 (55.1)	28 (31.8)	.0009
	L1–2	53 (44.9)	60 (68.2)	
Pn classification (n = 202)	Pn0	92 (80.0)	64 (73.6)	.28
	Pn1	23 (20.0)	23 (26.4)	
R classification (n = 199)	R0	106 (94.6)	82 (94.3)	.9828
	R1	6 (5.4)	5 (5.7)	
Tumor grade (n = 199)	G1	11 (9.6)	7 (8.3)	.4737
	G2	87 (75.7)	59 (70.2)	
	G3	17 (14.8)	18 (21.4)	
pM classification (n = 208)	pM0	116 (97.5)	74 (83.2)	.0003
	pM1	3 (2.5)	15 (16.7)	
Klintrup (n = 188)	1	59 (54.1)	39 (47.6)	.5215
	2	31 (28.4)	22 (26.8)	
	3	16 (14.7)	17 (20.7)	
	4	2 (1.8)	1 (1.2)	
Age (n = 208)	Mean ± SD	71.1 ± 11.9	69.7 ± 13.4	.4169
No. positive LN (n = 195)	Mean ± SD	2.32 ± 8.1	2.7 ± 5.3	.7079
Total no. LN (n = 195)	Mean ± SD	34.5 ± 20.9	36.3 ± 15.2	.49
Expansive % TBC (n = 190)	Mean ± SD	47.7 ± 34.9	44.1 ± 35.7	.4755
Tumor budding (n = 206)	Mean ± SD	68.2 ± 52.9	89.4 ± 61.7	.0084

It has been hypothesized that a subgroup of tumor buds are in a state of partial or full EMT, but studies to date, including some of our previous works, tend to make indirect conclusions. For example, tumor buds are reported to overexpress nuclear  $\beta$ -catenin, as well as numerous markers involved in EMT, and migration [21]. E-cadherin is disrupted from the membrane towards the invasion front and within tumor buds. Buds also rarely undergo apoptosis and overexpress

anoikis-resistance markers. They proliferate only little, in line with the “go or grow hypothesis”. Recently, we could show that tumor budding was significantly more frequent in colorectal cancers with a mesenchymal RNA profile, as outlined by the Consensus Molecular Subtypes (in revision, *Br J Cancer*). That tumor buds are heterogeneous is also reported. Stem cell markers may be over-expressed in a subset of buds, which leads to even worse clinical outcome [22]. Concerning tumor

**Table 4** Immunohistochemistry results comparing tumor-associated stroma (cancer-associated fibroblast) expression versus CK-positive stroma

	CK-negative				CK-positive stroma				McNemar
	Negative	%	Positive	%	Negative	%	Positive	%	P
CD90	2	3.6	53	96.4	6	10.9	49	89.1	.289
FAP	37	68.5	17	31.5	19	35.2	35	64.8	.003
SPARC	22	37.9	36	62.1	14	24.1	44	75.9	.134
COL11A1	20	33.9	39	66.1	30	50.8	29	49.2	.087
WT1	51	86.4	8	13.6	20	33.9	39	66.1	<.001
ZEB2	30	50	30	50	13	21.7	47	78.3	<.001
ZEB1	0	0	59	100	0	0	59	100	-
SNAIL1	41	67.2	20	32.8	33	54.1	28	45.9	.134
TWIST1	34	56.7	26	43.3	20	33.3	40	66.7	.009

budding, a caveat should be mentioned. Sectioning of glands may lead to a false impression of the presence of budding in some cases [23]. Bronsert and colleagues argue that single cell migration is negligible in colorectal cancers, but that nonetheless small clusters of cells reconstructed in 3D also show up-regulation of EMT markers such as ZEB and SNAIL and loss of E-cadherin from the membrane [24,25]. Studies using laser capture microdissection followed by RNA analysis give valuable insight into the tumor budding phenotype. Both in colorectal cancer and oral squamous cell carcinoma, more EMT-like profiles are found in regions containing budding in comparison to the center of the tumors [8,9]. Laser capture microdissection has been the closest method to analyzing single buds but this method is sometimes criticized since it may capture surrounding stroma. However, at least one study has additionally shown differences in miRNA expression in tumor buds and the surrounding stroma

suggesting not only epigenetic mechanisms involved in the tumor budding phenotype but also that laser capture is in fact an appropriate method to investigate this phenomenon [26]. This study here appears to be the first in colorectal cancer to identify the hybrid epithelial-mesenchymal phenotype using co-expression of CK and VIM that additionally can be attributed to tumor budding regions.

In a second step, we evaluated the significance of the presence of CK-positive stroma on tumor-related features. Tumors with positive expression of CK stroma were significantly associated with more aggressive features and nearly all such tumors were T3 and T4 cases. This is consistent with the findings from Chen and Borges who show that the proliferation of serosal stromal cells is associated with local peritoneal injury [12]. Our results show that in addition to this information, the staining of CK may have yet an additional role. Since this funky stroma was both CK and VIM positive and clearly

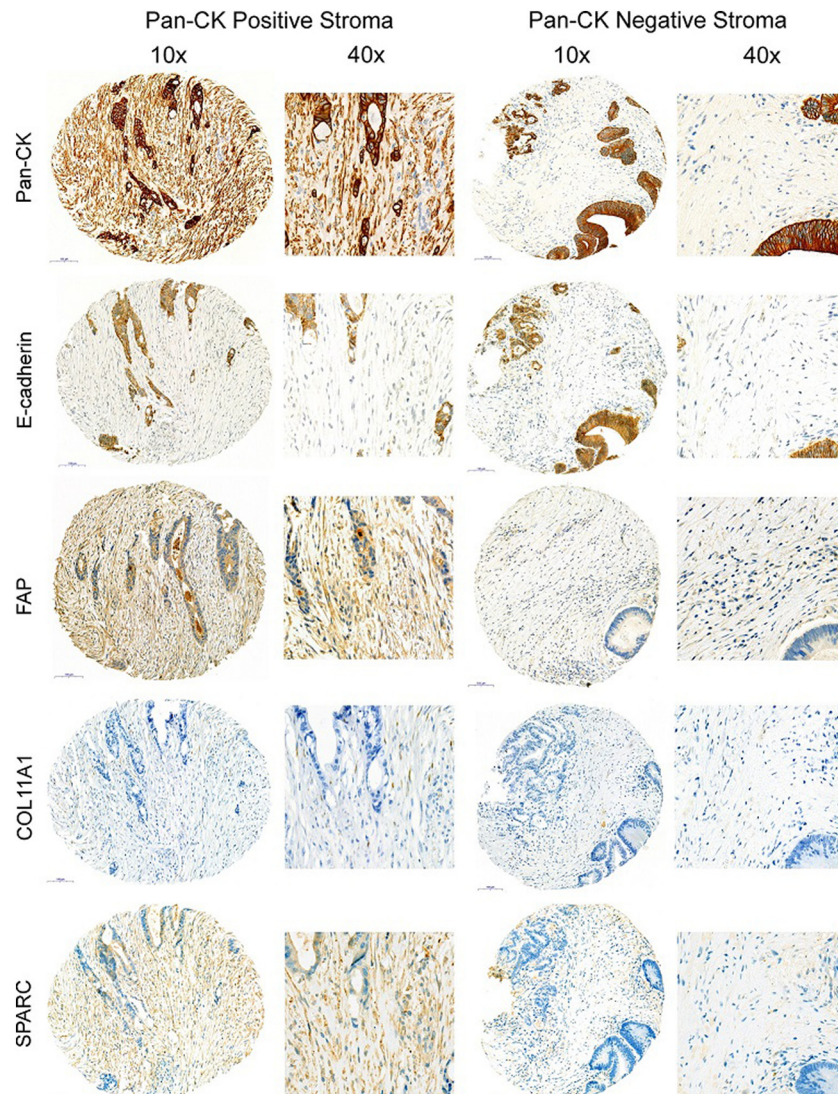


**Fig. 3** Representative images of immunohistochemistry stainings performed on matched samples in areas of CK-positive and CK-negative stroma. Low-power (10 $\times$ ) and high-power (40 $\times$ ) stains for Pan-CK, E-cadherin, FAP, COL11A1, and SPARC.

different from the surrounding tumor stroma, we set out to compare both types using markers of EMT (TWIST1, SNAIL1, ZEB1 and ZEB2), mesothelium (WT1) and classic markers of cancer-associated fibroblasts (CD90, FAP, SPARC). Results suggest that the CK-positive stroma is likely of mesothelial origin, but shows also characteristics of classic CAFs and up-regulation of EMT markers TWIST1 and ZEB2. These results show that these co-expressing cells are myofibroblasts (aSMA positive), likely originating from the mesothelium (WT1 positive), maintain their mesenchymal phenotype, through the activation of EMT transcription factors (Twist1 and Zeb2 positive), but also as well as acquire CAF specific markers (FAP positive). These results support the notion of mesothelial-mesenchymal transition (MMT) as a source of CAFs. During this process, mesothelial cells (MCs) are stimulated by tumor cells that acquire a myofibroblast-like phenotype and increase invasiveness and

promote vascularization. The accumulation of CAFs provides the tumor a suitable environment for progression [14,17]. Our results are in line with Sandoval et al [14], who demonstrated for the first time that CAFs derive from MCs through MMT. They showed not only the presence of CK-positive fibroblasts surrounding the tumor cells but WT1 expression, mesothelin, calretinin as mesothelial markers as well as the VEGF expression as angiogenesis marker since at advanced stages of peritoneal metastasis, angiogenesis is necessary for tumor progression. Our work highlights, the presence of these CAFs is associated with an array of aggressive tumor features including T stage (T3 and T4) according to MMT definition, as well as tumor budding and distant metastasis, which further supports this hypothesis. Unfortunately, survival data were not available for this cohort of patients.

In summary, tumor cells expressing epithelial and mesenchymal characteristics, defined by co-expression of CK and

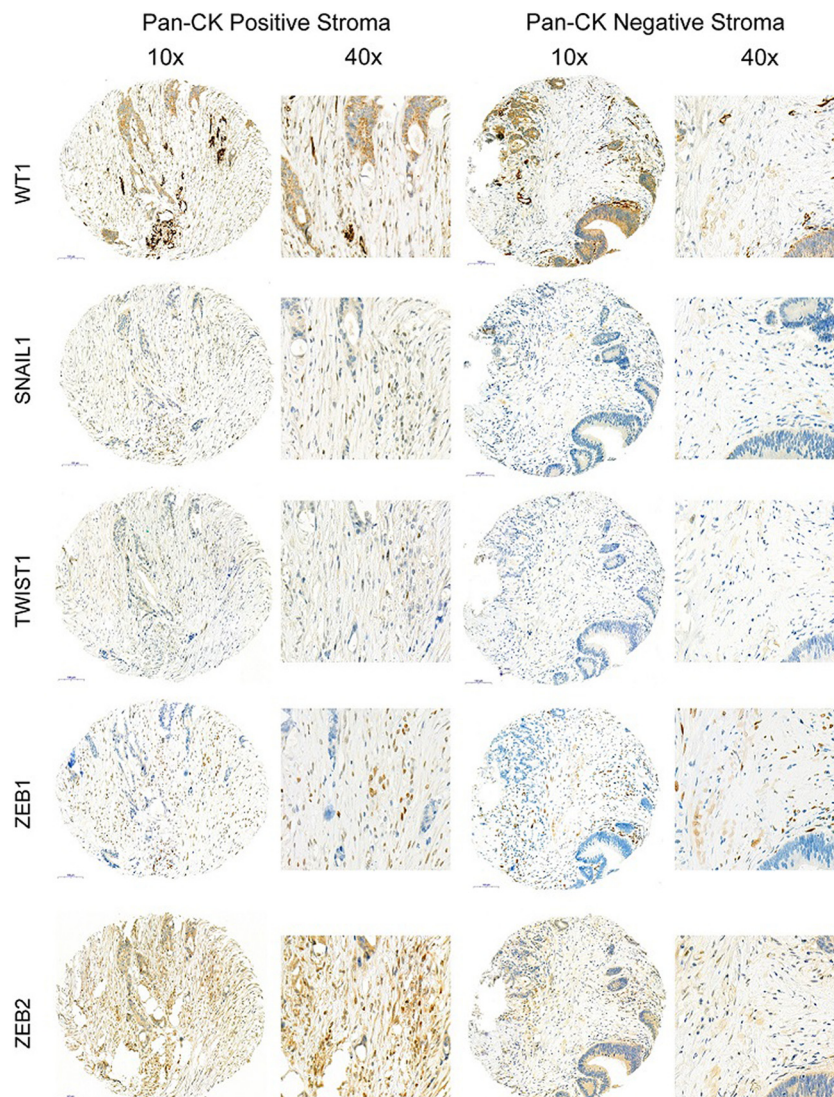


**Fig. 4** Representative images of immunohistochemistry stainings performed on matched samples in areas of CK-positive and CK-negative stroma. Low-power (10 $\times$ ) and high-power (40 $\times$ ) stains for WT1, SNAIL1, TWIST1, ZEB1, ZEB2.

VIM exist in colorectal cancer, albeit in very low number. We believe that these cells are the subgroup of tumor buds undergoing partial EMT. Moreover, CK-positive stroma is associated with an aggressive tumor phenotype and is an intermediate type of stroma with characteristics of CAFs with mesothelial origin. These CAFs may be important to consider as potential therapeutic targets.

## Supplementary data

Supplementary data to this article can be found online at <https://doi.org/10.1016/j.humpath.2019.02.002>.

## Acknowledgments

The authors would like to acknowledge R. Rosenberg, U. Nitsche and Rupert Langer for their help with case collection from Munich. Additional thanks go to the Translational Research Unit at the Institute of Pathology, University of Bern and FACS Facility of the DBMR, University of Bern for excellent technical assistance.

## References

- [1] Lugli A, Kirsch R, Ajioka Y, et al. Recommendations for reporting tumor budding in colorectal cancer based on the international tumor budding consensus conference (ITBCC) 2016. *Mod Pathol* 2017;30:1299-311.
- [2] Grigore AD, Jolly MK, Jia D, Farach-Carson MC, Levine H. Tumor budding: the name is EMT. *Partial EMT. J Clin Med* 2016;5.
- [3] Kohler I, Bronsert P, Timme S, et al. Detailed analysis of epithelial-mesenchymal transition and tumor budding identifies predictors of long-term survival in pancreatic ductal adenocarcinoma. *J Gastroenterol Hepatol* 2015;30(Suppl. 1):78-84.
- [4] Galvan JA, Zlobec I, Wartenberg M, et al. Expression of E-cadherin repressors SNAIL, ZEB1 and ZEB2 by tumour and stromal cells influences tumour-budding phenotype and suggests heterogeneity of stromal cells in pancreatic cancer. *Br J Cancer* 2015;112:1944-50.
- [5] Jass JR, Barker M, Fraser L, et al. Leggett BA. APC mutation and tumour budding in colorectal cancer. *J Clin Pathol* 2003;56:69-73.
- [6] Knudsen KN, Lindebjerg J, Nielsen BS, Hansen TF, Sorensen FB. MicroRNA-200b is downregulated in colon cancer budding cells. *PLoS One* 2017;12:e0178564.
- [7] Trumpi K, Frenkel N, Peters T, et al. Macrophages induce "budding" in aggressive human colon cancer subtypes by protease-mediated disruption of tight junctions. *Oncotarget* 2018;9:19490-507.
- [8] De Smedt L, Palmans S, Andel D, et al. Expression profiling of budding cells in colorectal cancer reveals an EMT-like phenotype and molecular subtype switching. *Br J Cancer* 2017;116:58-65.
- [9] Jensen DH, Dabelsteen E, Specht L, et al. Molecular profiling of tumour budding implicates TGFbeta-mediated epithelial-mesenchymal transition as a therapeutic target in oral squamous cell carcinoma. *J Pathol* 2015;236:505-16.
- [10] Guinney J, Dienstmann R, Wang X, et al. The consensus molecular subtypes of colorectal cancer. *Nat Med* 2015;21:1350-6.
- [11] Koelzer VH, Assarzadegan N, Dawson H, et al. Cytokeratin-based assessment of tumour budding in colorectal cancer: analysis in stage II patients and prospective diagnostic experience. *J Pathol Clin Res* 2017;3:171-8.
- [12] Chen JH, Borges M. Histopathology and enhanced detection of tumor invasion of peritoneal membranes. *PLoS One* 2017;12:e0173833.
- [13] Kojima M, Higuchi Y, Yokota M, et al. Human subperitoneal fibroblast and cancer cell interaction creates microenvironment that enhances tumor progression and metastasis. *PLoS One* 2014;9:e88018.
- [14] Sandoval P, Jimenez-Heffernan JA, Rynne-Vidal A, et al. Carcinoma-associated fibroblasts derive from mesothelial cells via mesothelial-to-mesenchymal transition in peritoneal metastasis. *J Pathol* 2013;231:517-31.
- [15] Kalluri R, Zeisberg M. Fibroblasts in cancer. *Nat Rev Cancer* 2006;6:392-401.
- [16] Polanska UM, Orimo A. Carcinoma-associated fibroblasts: non-neoplastic tumour-promoting mesenchymal cells. *J Cell Physiol* 2013;228:1651-7.
- [17] Rynne-Vidal A, Jimenez-Heffernan JA, Fernandez-Chacon C, Lopez-Cabrera M, Sandoval P. The mesothelial origin of carcinoma associated-fibroblasts in peritoneal metastasis. *Cancers (Basel)* 2015;7:1994-2011.
- [18] Karamitopoulou E, Zlobec I, Kolzer V, et al. Proposal for a 10-high-power-fields scoring method for the assessment of tumor budding in colorectal cancer. *Mod Pathol* 2013;26:295-301.
- [19] Zlobec I, Suter G, Perren A, Lugli A. A next-generation tissue microarray (ngTMA) protocol for biomarker studies. *J Vis Exp* 2014;91.
- [20] Fabbri F, Carloni S, Zoli W, et al. Detection and recovery of circulating colon cancer cells using a dielectrophoresis-based device: KRAS mutation status in pure CTCs. *Cancer Lett* 2013;335:225-31.
- [21] Dawson H, Lugli A. Molecular and pathogenetic aspects of tumor budding in colorectal cancer. *Front Med (Lausanne)* 2015;2:11.
- [22] Hostettler L, Zlobec I, Terracciano L, Lugli A. ABCG5-positivity in tumor buds is an indicator of poor prognosis in node-negative colorectal cancer patients. *World J Gastroenterol* 2010;16:732-9.
- [23] Prall F, Ostwald C, Linnebacher M. Tubular invasion and the morphogenesis of tumor budding in colorectal carcinoma. *HUM PATHOL* 2009;40:1510-2.
- [24] Bronsert P, Enderle-Ammour K, Bader M, et al. Cancer cell invasion and EMT marker expression: a three-dimensional study of the human cancer-host interface. *J Pathol* 2014;234:410-22.
- [25] Enderle-Ammour K, Bader M, Ahrens TD, et al. Form follows function: morphological and immunohistological insights into epithelial-mesenchymal transition characteristics of tumor buds. *Tumour Biol* 2017;39:1010428317705501.
- [26] Karamitopoulou E, Haemmig S, Baumgartner U, Schlup C, Wartenberg M, Vassella E. MicroRNA dysregulation in the tumor microenvironment influences the phenotype of pancreatic cancer. *Mod Pathol* 2017;30:1116-25.
- [27] Zlobec I, Suter G, Perren A, Lugli A. A next-generation tissue microarray (ngTMA) protocol for biomarker studies. *J Vis Exp* 2014(91).
- [28] Trinh A, Ladrach C, Dawson HE, et al. Tumour budding is associated with the mesenchymal colon cancer subtype and RAS/RAF mutations: a study of 1320 colorectal cancers with Consensus Molecular Subgroup (CMS) data. *Br J Cancer* 2018;119:1244-51.